Catalysis Today 232 (2014) 89–98

Contents lists available at ScienceDirect

Catalysis Today

journal homepage: www.elsevier.com/locate/cattod

Selective hydrogenation of biomass-derived 5-hydroxymethylfurfural (HMF) to 2,5-dimethylfuran (DMF) under atmospheric hydrogen pressure over carbon supported PdAu bimetallic catalyst

Shun Nishimura, Naoya Ikeda, Kohki Ebitani*

School of Materials Science, Japan Advanced Institute of Science and Technology, 1-1, Asahidai, Nomi, Ishikawa 923-1292, Japan

ARTICLE INFO

Article history:
Received 16 July 2013
Received in revised form
22 September 2013
Accepted 2 October 2013
Available online 29 October 2013

Keywords:
Hydrogenation
PdAu bimetallic catalyst
Bio-fuel
2,5-Dimethylfuran

ABSTRACT

Hydrogenation of 5-hydroxymethylfurfural (HMF) to 2,5-dimethylfuran (DMF) was examined by Pd_xAu_y/C catalysts prepared with various Pd/Au molar ratio (x/y) in the presence of hydrochloric acid (HCl) under an atmospheric hydrogen pressure. Bimetallic Pd_xAu_y/C catalysts had a significant activity for a selective hydrogenation of HMF toward DMF comparing to monometallic Pd/C and Au/C catalysts. To clarify the novelty of Pd_xAu_y/C catalysts, characterizations by using X-ray diffraction (XRD), X-ray photoelectron spectroscopy (XPS), X-ray absorption spectra (XAFS), a transmission electron microscopy (TEM) and other analytical techniques were studied. XPS and X-ray absorption near-edge structure (XANES) analyses indicated that there was the charge transfer phenomenon from Pd to Au atoms in Pd_xAu_y/C. Existence of PdAu alloy structures in Pd_xAu_y/C was expected by XRD, TEM and extended X-ray absorption fine structure (EXAFS) analyses. Accordingly, we concluded that PdAu alloys supported carbon exhibited a good catalytic performance for a selective hydrogenation of HMF to DMF using an atmospheric hydrogen pressure.

1. Introduction

Fossil energies such as natural gas, coal and petroleum dominate approximately 80% in primary energy consumption estimated by sources [1]. This excessive reliance on fossil fuels in the world has serious reservations about their depletion and green house emission. Now, with increasing the demand for environmental concerns about global warming, the development of renewable and environmentally friendly energy sources have been a hot and an important topic in these decades [2,3]. The energy-efficient processes for the sustainable production of fuels derived from biomass resources such as bio-ethanol, biodiesel fuel (BDF) and liquid alkanes have also attracted attention over the year [4].

5-Hydroxymethylfurfural (HMF), obtained by dehydration of monosaccharides, is considered to be the most promising important intermediate for the synthesis of a wide variety of chemicals and alternative fuels based on bio-refinery [5]. To upgrade furanic compounds toward bio-fuels, hydrogenation is the most versatile reaction. 2,5-Dimethylfuran (DMF) is known as one of the potential transportation fuels due to its high energy density (30 kJ cm^{-3}) and a high research octane number (RON = 119), these are similar values to that of gasoline which possesses 34 kJ cm^{-3} and RON = 89–96, respectively. Moreover, a low solubility in water (2.3 g L^{-1}) is superior to miscible ethanol, and it enables use as the blend fuel.

For the gas-phase converter system affording to DMF, Dumesic et al. designed the copper/ruthenium (CuRu/C) catalyzed biphasic reactor with hydrochloric acid (HCl) and sodium chloride (NaCl) [6]. They also reported that the Cu_3Ru_1/C catalyst exhibited 71% yield of DMF from 5 wt% HMF at 220 °C under pressured hydrogen (6.8 atm H_2) in batch reactor. Chidambaram and Bell proposed the catalytic conversion of glucose to DMF with a following two-step reaction; dehydration of glucose to HMF using heteropoly acid (12-molybdophosphoric acid) in ionic liquid and successive hydrogenation of HMF to DMF with Pd/C catalyst [7]. In their report, the Pd/C showed 15% yield of DMF *via* hydrogenation reaction of HMF (1 mmol) in ionic liquid/acetonitrile at 120 °C under 62 atm of H_2. Hydrogenation of HMF toward BHMF over subnano-ordered Au cluster-supported Al_2O_3 (140 °C, 38 atm H_2) [8] or toward 2,5-bis(hydroxymethyl)tetrahydrofuran (DHTHF) over Ru, Pd or Pt-supported catalysts (130 °C, 27 atm H_2) [9], and syntheses of DHTHF and 2,5-dimethyltetrahydrofuran (DMTHF) from various saccharides over $RhCl_3$ catalyst (80–160 °C, 20 atm H_2) [10] were also examined under pressured H_2 condition, previously.

Under an atmospheric H_2 condition, hydrogenation of HMF toward DMF has mainly catalyzed by Pd-supported carbon in the presence of strong acidic media. van Bekkum et al. investigated the hydrogenation of HMF to DMF by using a combination of Pd/C catalyst and HCl as an activator in alcohol solvents [11]. They

* Corresponding author. Tel.: +81 761 51 1610; fax: +81 761 51 1149.
E-mail address: ebitani@jaist.ac.jp (K. Ebitani).

0920-5861/$ – see front matter © 2013 Elsevier B.V. All rights reserved.
http://dx.doi.org/10.1016/j.cattod.2013.10.012

achieved 36% yield of DMF from HMF at 60 °C under 1 atm of H_2. In the presence of alcohol, the reaction between alcohol solvent and furanyl ketone to ether, *ex.* the monopropyl ether of 2,5-bis(hydroxymethyl)furan (BHMF) formation with 1-propanol and BHMF, is an expected intermediary reaction step. Notably, Rauchfuss and co-workers succeeded >95% yield of DMF through the hydrogenation of HMF in the presence of Pd/C, sulfuric acid (H_2SO_4) and formic acid (FA) in refluxing tetrahydrofuran (THF) [12,13]. Their key strategy is the multirole of FA as an acid catalyst, solvent, a source of hydrogen (H_2) and a reagent for the dehydrogenation of furanylmethanols to produce the formate ester intermediate of BHMF and 2-hydroxymethyl-5-methylfuran (HMMF). Saha and co-workers also tried the synthesis of DMF from different biomass sources by using FA with H_2SO_4 and Ru/C catalyst in refluxing THF, and they afforded 30% yield of DMF from fructose [14]. Following to these approaches, production of the ester intermediate such as propyl ether and formate ester is one of the crucial points for enhancement of hydrogenolysis step.

Herein, we studied the hydrogenation of HMF toward DMF over PdAu bimetallic catalyst under an atmospheric H_2 pressure. The PdAu types of bimetallic catalyst has been well-known as an active bimetallic nanocatalyst for aerobic oxidation of alcohols [15–18], direct synthesis of hydrogen peroxide (H_2O_2) from H_2 and O_2 [19,20], Suzuki–Miyaura reactions [21,22], dehalogenation [23], and so on, these achievements have made tremendous performances comparing to that over the monometallic Au or Pd catalytic system. We found that the PdAu alloy particles supported on carbon promoted the hydrogenolysis step, and it served good yield of DMF by the selective hydrogenation of HMF under mild reaction conditions.

2. Experimental

2.1. Materials

Fructose, hydrochloric acid (HCl, 35.0 wt%), sulfuric acid (H_2SO_4, 96.0 wt%), ruthenium(III) chloride trihydrate ($RuCl_3{\cdot}3H_2O$), potassium chloride (KCl) were obtained by KANTO Chemical Co., Inc. Glucose, carbon (Norite "SX plus", surface area is about 800 $m^2\,g^{-1}$) [24], palladium chloride ($PdCl_2$), tetrachloroauric(III) acid tetrahydrate ($HAuCl_4{\cdot}4H_2O$), hexachloroplatinic(IV) acid hexahydrate ($H_2PtCl_6{\cdot}6H_2O$), sodium borohydride ($NaBH_4$), dehydrated tetrahydrofuran (THF), formic acid (FA, 99 wt%), 2,5-dimethylfuran (DMF) and 2-methylfuran (2-MF) were purchased from WAKO Pure Chemical Industries, Ltd. Tagatose, 5-hydroxymethylfurfural (HMF), 2,5-dimethyltetrahydrofuran (DMTHF), furfural and 5-methylfurfural (5-MF) were received from Sigma–Aldrich Co. Llc. Galactose and naphthalene were served by Tokyo chemical industry (TCI) Co. Ltd. 5-Methylfurfurylalcohol (MFA), 2,5-bis(hydroxymethyl)furan (BHMF) and 2,5-bis(hydroxymethyl)tetrahydrofuran (DHTHF) were bought from Toronto Research Chemicals (TRC) Inc.

2.2. Preparation of the Pd_xAu_y bimetallic nanoparticles supported carbon catalyst

Monometallic or bimetallic nanoparticles-supported catalysts were prepared by $NaBH_4$ reduction method referred to the previous report [25] with some modifications. For instance, the preparation method of palladium and gold-supported carbon catalyst (Pd_xAu_y/C) was as follows. First, the carbon support (0.47 g) was dispersed into the mixed solution of deionized water (55 ml) and 2-propanol (55 ml). Subsequently, $PdCl_2$ (*a* mmol), KCl (1.0 g) and $HAuCl_4{\cdot}4H_2O$ (*b* mmol) were added into the solution. After an ultrasonic treatment for 5 min and a further vigorous stirring for 1 h at room temperature, the $NaBH_4$ reductant was gradually dropped into the above mixture of Pd^{2+} and Au^{3+} ions to reduce, deposit and stabilize bimetallic ions onto the carbon surface. The produced precipitate was filtered, washed with 1 L of deionized water, and dried in oven at 100 °C for overnight. Concentration of the sum of Pd and Au elements was kept constant as 0.94 mmol g^{-1} for Pd_xAu_y/C catalysts ($x+y=100$). $Pd_{50}Ru_{50}$/C and $Pd_{50}Pt_{50}$/C were also prepared by the same method with $RuCl_3{\cdot}3H_2O$ and $H_2PtCl_6{\cdot}6H_2O$, respectively, instead of the mixture of $PdCl_2$ and KCl. On the other hand, the concentration of 0.47 mmol g^{-1} was applied for the preparation of monometallic catalysts such as Pd_{50}/various supports, Ru_{50}/C and Pt_{50}/C.

2.3. Hydrogenation of HMF to DMF with atmospheric hydrogen (H_2)

Hydrogenation reactions were performed in 60 mL volume of a Schlenk flask. Briefly, HMF (1.0 mmol) was dissolved into THF (10 mL) solvent, then Pd_xAu_y/C (31.3 mg) catalyst and HCl (0.17 mmol) acidic media were added into the mixture. A balloon (4 L) fulfilled with H_2 gas was attached with the Schlenk flask during the reaction heated in the oil bath at 60 °C with a vigorous stirring (550 rpm). The products were analyzed by a GC chromatography (Shimadzu GC-2014) equipped with a capillary column (Agilent J&W GC DB-1; 0.320 mm × 50 m) and a flame ionization detector (FID) under ramping temperature from 40 to 280 °C. The naphthalene was used as an internal standard. Retention times in GC-FID determined by injections of the commercially available chemicals were following orders; 2-MF (3.44 min), THF (3.70 min), DMF (4.89 min), DMTHF (4.8 min and 5.01 min) [26], furfural (7.94 min), furfuryl alcohol (9.38 min), 5-MF (14.55 min), MFA (14.81 min), naphthalene (19.47 min), DHTHF (19.58 min), HMF (19.70 min), BHMF (20.77 min).

2.4. Characterization of Pd_xAu_y/C catalysts

X-ray diffraction (XRD) patterns were obtained by a Smart-Labo X-ray diffractometer (Shimadzu) using Cu-Kα radiation at 40 kV and 30 mA in the range of 2θ from 30° to 90° in 0.01° resolution. X-ray photoelectron spectroscopy (XPS) was measured by a AXIS-ULTRA DLD spectrometer (Shimadzu–Kratos) equipped with a Al target accelerated at 15 kV and 10 mA. The binding energies of obtained spectra were calibrated with the C 1*s* speak at 284.5 eV. X-ray absorption spectra (XAFS) in Au L_3-edge and Pd *K*-edge were recorded at a BL5S1 of Aichi Synchrotron Radiation Research Center (2nd period, 2013) and a BL01B1 of SPring-8 in the Japan Synchrotron Radiation Research Institute (JASRI) (Proposal No. 2012B1610) with a quick XAFS scanning mode. All samples were grained and pressed to a pellet (Ø = 10 mm). The energy for Au L_3-edge and Pd *K*-edge XAFS spectra were adjusted at the edges of Cu foil (8.9800 keV) and Pd foil (24.347 keV), respectively. Double Si(1 1 1) single crystals and double Si(3 1 1) single crystals were used for division of energy in Au L_3-edge and Pd *K*-edge, respectively. The obtained spectra were analyzed with the REX2000 software (ver. 2.5.92, Rigaku). Fourier transformation (FT) was applied in the range of k = 3–13 $Å^{-1}$ in each EXAFS spectrum. The curve-fitting analyses were performed in the range of k = 4–12 $Å^{-1}$ using the inverse FTs in R = 1.841–3.283 Å for Au L_3-edge and R = 1.811–3.161 Å for Pd *K*-edge. Morphologies of the catalysts were observed by a transmission electron microscopy (TEM) with Hitachi H-7650 at 100 kV. The size distribution was produced by randomly counting up of 500 particles. Scanning TEM-high angle annular dark field (STEM-HAADF) image with an energy dispersive X-ray spectroscopy (EDS) elemental mapping was carried out by a JEOL JEM-ARM200F instrument operated at 200 kV with the support of Nanotechnology Platform Program in JAIST of

Table 1
Synthesis of DMF *via* hydrogenation of HMF over the precious metal-supported catalysts.[a]

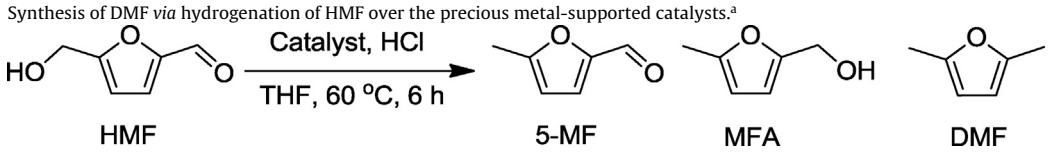

Entry	Catalyst[c]	Conversion of HMF/%	Yield/%		
			5-MF	MFA	DMF
1	Pd_{50}/C	>99, 91[b]	0, 4[b]	0, 11[b]	>99, 66[b]
2	$Pd_{50}Au_{50}/C$	>99, >99[b]	0, 2[b]	0, 2[b]	>99, 96[b]
3	$Pd_{50}Pt_{50}/C$	>99, 67[b]	0, 4[b]	0, 5[b]	93, 31[b]
4	$Pd_{50}Ru_{50}/C$	98	0	0	62
5	Ru_{50}/C	65	0	0	4
6	Pt_{50}/C	61	0	0	Trace
7	Au_{50}/C	53	0	0	0
8	Blank	47	0	0	0

[a]Reaction conditions: HMF (0.5 mmol, [b]1.0 mmol), THF (10 ml), HCl (0.17 mmol), catalyst (62.5 mg, [b]31.3 mg), H_2 balloon (purge), temp. (60 °C), time (6 h, [b]12 h). [c]Concentration of the monometallic X_{50}/support is 0.47 mmol g^{-1} whereas that of the $X_{50}Y_{50}$/support is totally 0.94 mmol g^{-1} with a molar ratio of X/Y = 50/50.

the Ministry of Education, Culture, Sports, Science and Technology (MEXT), Japan.

3. Results and discussion

3.1. Screening of Pd-based heterogeneous catalysts for selective hydrogenation of HMF to DMF

Table 1 shows the activities for hydrogenation of HMF to DMF over Pd, Au, Pt and/or Ru-supported carbon catalysts. Ru_{50}/C, Pt_{50}/C and Au_{50}/C were inactive for DMF synthesis (entries 5–7) whereas Pd_{50}/C gave a good activity affording to DMF (entry 1) among monometallic catalysts. To accelerate the catalytic activity of Pd_{50}/C catalyst, effect of second elements such as Au, Pt or Ru into Pd catalyst was also examined. Additional Pt and Ru decreased the activity of Pd_{50}/C (>99% yield) to 93% and 62%, respectively (entries 3 and 4). While the Au combined with Pd atoms, $Pd_{50}Au_{50}/C$, showed a positive effect for the activity, it was observed that 66% yield over Pd_{50}/C changed to 96% over $Pd_{50}Au_{50}/C$ in 1.0 mmol scale reaction (entries 1 and 2).

Effects of acidic co-catalyst and support for the synthesis of DMF from HMF hydrogenation reaction by Pd-supported catalysts were investigated (Table 2). Instead of carbon support, acidic compounds such as SiO_2, β-zeolite, Amberlyst-15 and α-Al_2O_3 were also compared as a support for Pd (Each morphologies were shown in Fig. S1). Pd_{50}/Amberlyst-15 and Pd_{50}/α-Al_2O_3 showed small activities (entries 7 and 8) whereas Pd_{50}/SiO_2 and Pd_{50}/β-zeolite gave mild activities (entries 5 and 6), however, their activities were not superior to that of Pd_{50}/C (entry 1). Several peaks in GC chromatograph were appeared in the range of retention time at 20–26 min in cases of Pd_{50}/SiO_2 and Pd_{50}/β-zeolite. Pd_{50}/Amberlyst-15 and Pd_{50}/β-zeolite also indicated a new single peak at 18.1 min due to the 2,5-hexanedione formation which was produced by the hydrolysis reaction of DMF, though this product was not observed in Pd_{50}/C. Therefore, acidic supports may cause the side pathways, *ex.* a ring-opening of DMF. It was reported that the ring opening by hydrolytic cleavage of the furanic C—O bond is typically promoted with Brønsted acid sites of aluminosilicates and ion-exchange resins [27,28]. As shown in Table 2, the differences of acidity seemed to influence the catalytic activities. It indicated that a co-existence of strong acidic media such as HCl and H_2SO_4 was required for a selective hydrogenation of HMF toward DMF, and the HCl was found to be the best acid for a high efficiency (entries 1–4). Lange et al. reported that not only the strong acidity ($pK_a < -5$) but also chloride ions were needed for a selective and an effective hydrogenation of furanic compounds because the HCl acted as the co-catalyst which prevented an undesired ring-hydrogenation and enhanced the hydrogenolysis step by formation of an active chlorinated intermediate through nucleophilic substitution on the alcohol groups [29]. Combined with these results discussed in Tables 1 and 2, the PdAu/C catalyst in the presence of HCl acidic media promoted an efficient hydrogenation of HMF to DMF even under mild reaction conditions (60 °C, atmospheric H_2).

Table 2
Effect of support and acid for the synthesis of DMF *via* hydrogenation of HMF over the Pd-supported catalysts.[a]

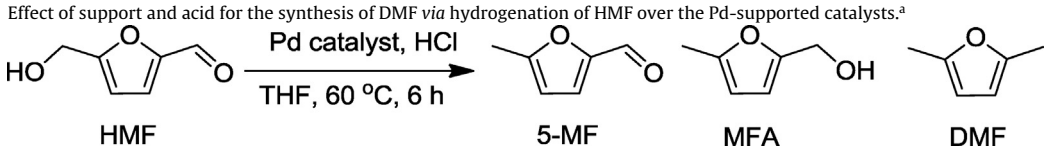

Entry	Catalyst[c]	Conversion of HMF/%	Yield/%		
			5-MF	MFA	DMF
1	Pd_{50}/C	91	4	11	66
2	Pd_{50}/C[b]	>99	0	0	50
3	Pd_{50}/C[c]	66	0	6	6
4	Pd_{50}/C[d]	41	<1	5	3
5	Pd_{50}/SiO_2	83	6	12	40
6	Pd_{50}/β-zeolite	91	5	0	29
7	Pd_{50}/Amberlyst-15	60	7	0	8
8	Pd_{50}/α-Al_2O_3	63	7	6	6
9	Blank	38	0	0	0

[a]Reaction conditions: HMF (1.0 mmol), THF (10 ml), HCl (0.17 mmol), catalyst (31.3 mg, Pd = 0.47 mmol g^{-1}), H_2 balloon (purge), temp. (60 °C), time (12 h). Instead of HCl, [b]H_2SO_4 (0.085 mmol), [c]FA (0.17 mmol) and [d]without acid were used for each runs, respectively.

Table 3
Synthesis of DMF *via* hydrogenation of HMF over the Pd_xAu_y/C catalysts with various Pd/Au molar ratios.[a]

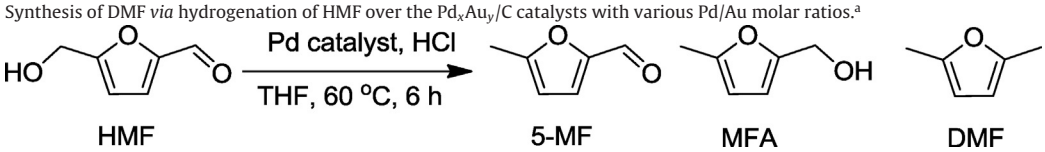

Entry	Catalyst	Conversion of HMF/%	Yield/%		
			5-MF	MFA	DMF
1	Pd_{100}/C	89	4	12	60
2	$Pd_{70}Au_{30}$/C	96	4	7	79
3	$Pd_{60}Au_{40}$/C	95	5	5	88
4	$Pd_{50}Au_{50}$/C	>99, 81[b]	2, 4[b]	2, 4[b]	96, 55[b]
5	$Pd_{40}Au_{60}$/C	>99, 77[b]	4, 4[b]	2, 3[b]	94, 41[b]
6	$Pd_{30}Au_{70}$/C	96	6	3	84
7	Au_{100}/C	32	0	0	0
8	Pd_{50}/C[c]	91	4	11	66
9	Au_{50}/C[c]	51	0	0	0
10	Pd_{50}/C + Au_{50}/C[d]	81	6	8	51
11	Blank	38	0	0	0

[a]Reaction conditions: HMF (1.0 mmol, [b]3.0 mmol), THF (10 ml), HCl (0.17 mmol), catalyst (31.3 mg, Pd + Au = 0.94 mmol g^{-1}, [c]Pd or Au = 0.47 mmol g^{-1}), H_2 balloon (purge), temp. (60 °C), time (12 h, [b]36 h), [d]physical mixture of Pd_{50}/C (15.5 mg) and Au_{50}/C (15.5 mg).

3.2. Hydrogenation of HMF to DMF over Pd_xAu_y/C catalysts

To study the contribution of Pd/Al molar ratio, the hydrogenation of HMF to DMF was examined over Pd_xAu_y/C catalysts prepared with various Pd/Au molar ratio (*x*/*y*) (Table 3). It was observed that a gradual increase of Au contents in Pd_xAu_y/C induced a gradual increase of activity at *y* = 0–50 (entries 1–4), thereafter, the activities were decreasing at *y* = 50–100 (entries 5–7). Interestingly, the physical mixture of Pd_{50}/C and Au_{50}/C showed a lower activity (51% yield, entry 10) than that of bimetallic $Pd_{50}Au_{50}$/C (96% yield, entry 4). The $Pd_{50}Au_{50}$/C also presented 55% yield of DMF in 3 mmol scale (entry 4*b*), and it was very notable in comparison with previous reports because the significant decrease of metal amount (Pd and/or Au) was achieved with a good activity (see Table S1). These results indicated that the as-prepared PdAu/C catalysts had some interactions between Pd and Au atoms which produced different effects on active sites from monometallic Pd/C and Au/C.

Time-courses of the hydrogenation of HMF toward DMF over monometallic Pd/C and bimetallic PdAu/C catalysts were shown in Fig. 1. In both cases, the production of DMF gradually proceeded with consuming HMF. 5-MF and MFA were obtained as the intermediate species. BHMF was also detected but it was trace amount in all steps (not plotted in Fig. 1). Additionally, the over-hydrogenation products such as DHTHF, DMTHF and the 2,5-hexanedione were not detected (0% yield in all step). Therefore, the hydrogenation of HMF to DMF under our experimental conditions mainly involves two-step; the reduction of the aldehyde group to alcohol group, and the hydrogenolysis of the hydroxyl group (Scheme 1). It was indicated that the rate of DMF production over PdAu/C was faster than Pd/C.

In order to get more insights of catalytic enhancement phenomena over PdAu/C catalyst, time-courses of hydrogenation of 5-MF and MFA toward DMF were also monitored (Figs. 2 and 3). The transformation of 5-MF to DMF occurred through the MFA formation in both cases. Interestingly, the life-time of MFA over PdAu/C seemed to be shorter than that over Pd/C (Fig. 2). Following to the result in Fig. 3, the reaction from MFA to DMF became faster in the case of PdAu/C. Therefore, the hydrogenolysis step, converting MFA to DMF, during hydrogenation of HMF toward DMF seems to be enhanced by the addition of Au into Pd atoms. That is because the yield of MFA was smaller than 5-MF during the reaction over PdAu/C though Pd/C remained MFA in Fig. 1. In comparison

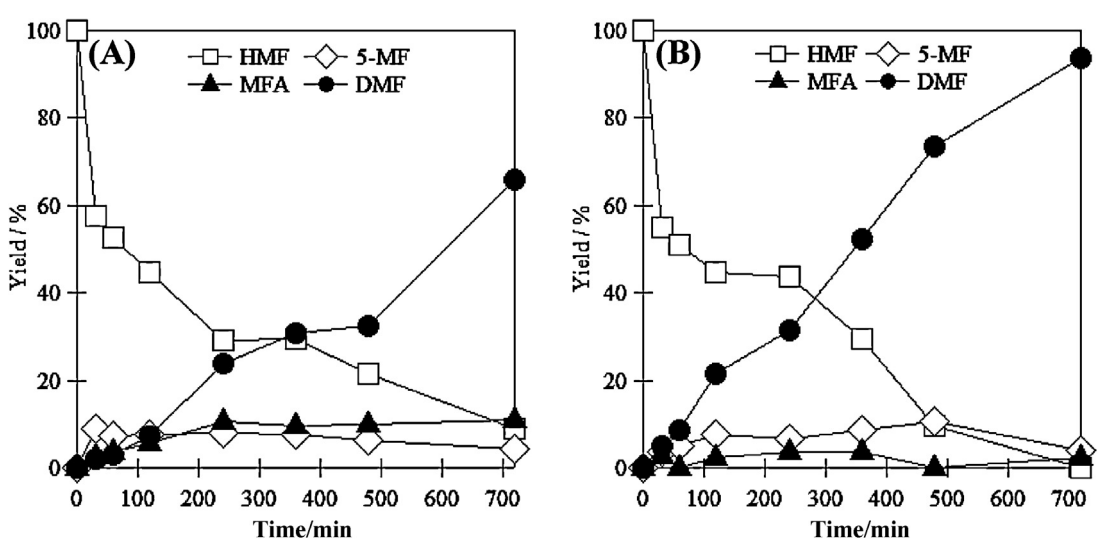

Fig. 1. Time course of the hydrogenation of HMF toward HMF over (A) Pd_{50}/C and (B) $Pd_{40}Au_{60}$/C catalysts. *Reaction conditions*; HMF (1.0 mmol), THF (10 ml), HCl (0.17 mmol), catalyst (31.3 mg), H_2 balloon (purge), 60 °C.

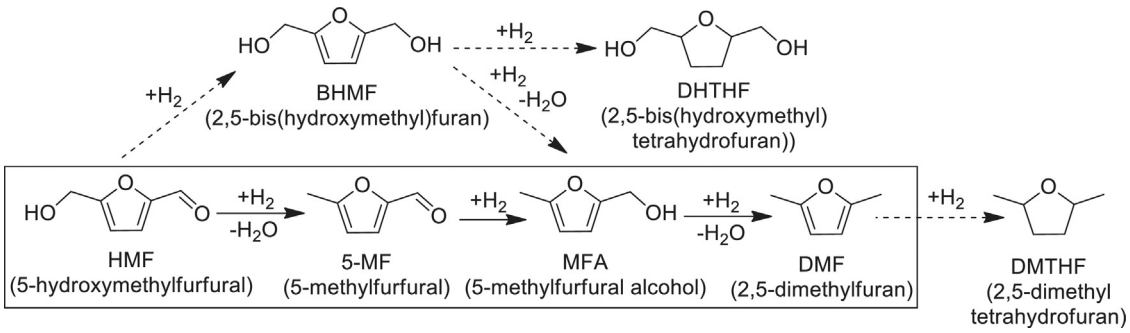

Scheme 1. Reaction pathway for the hydrogenation of HMF toward DMF.

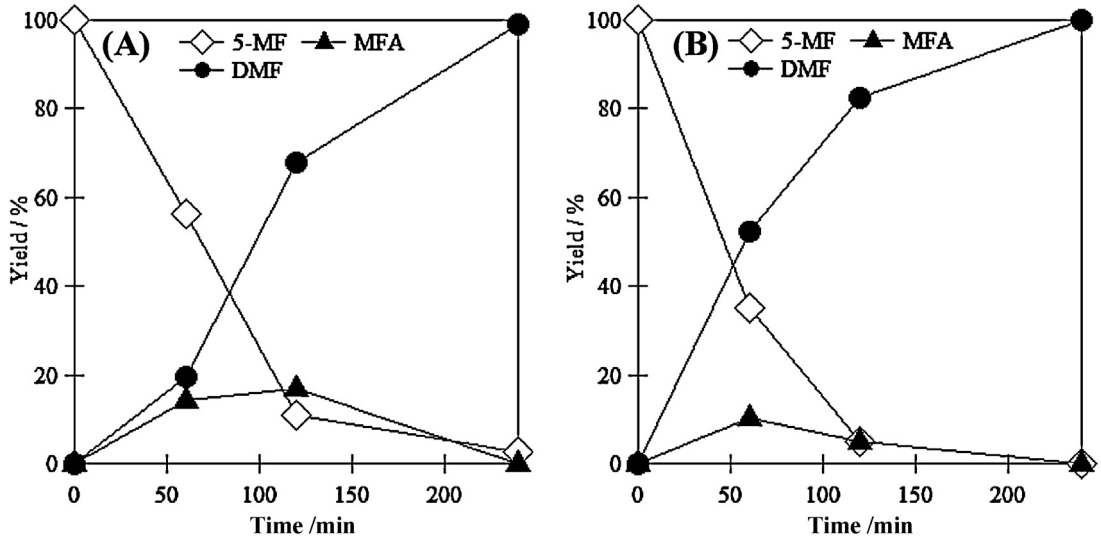

Fig. 2. Time course of the hydrogenation of 5-MF into DMF over (A) Pd_{50}/C and (B) $Pd_{40}Au_{60}$/C catalysts. *Reaction conditions*; substrate (0.5 mmol), THF (10 ml), HCl (0.17 mmol), catalyst (31.3 mg), H_2 balloon (purge), 60 °C.

between Figs. 2 and 3, it was also ascertained that the consumption rate of 5-MF was slower than MFA in both cases of Pd/C and PdAu/C. Furthermore, on the other hand, focusing on the production rate of DMF gave the information that DMF production from 5-MF was faster than that from MFA; *i.e.* the production of DMF through the hydrogenation of MFA seems to be saturated in Fig. 3. We believed that excess number of MFA adsorbed on the surface of Pd may inhibit the formation of DMF. [30]

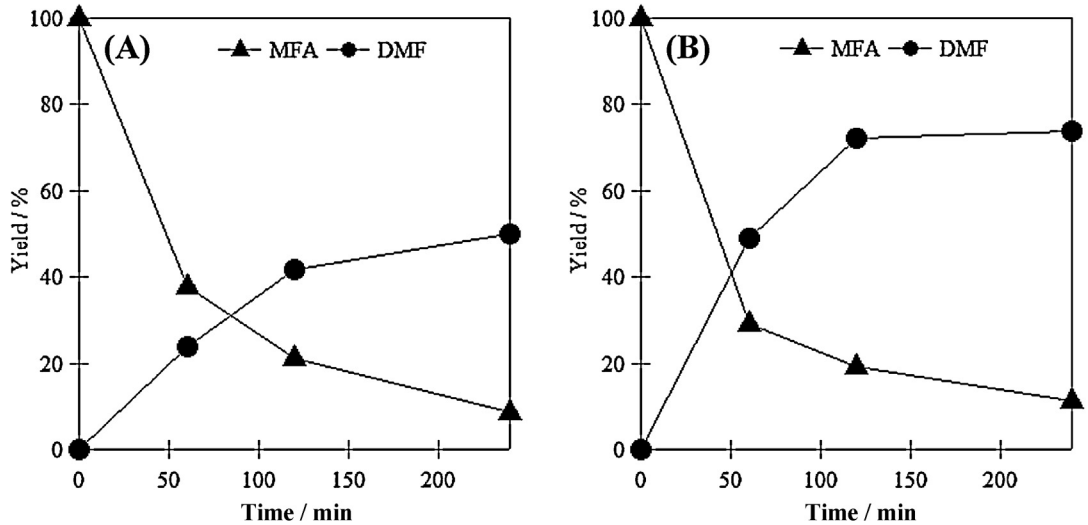

Fig. 3. Time course of the hydrogenation of MFA into DMF over (A) Pd_{50}/C and (B) $Pd_{40}Au_{60}$/C catalysts. *Reaction conditions*; substrate (0.5 mmol), THF (10 ml), HCl (0.17 mmol), catalyst (31.3 mg), H_2 balloon (purge), 60 °C.

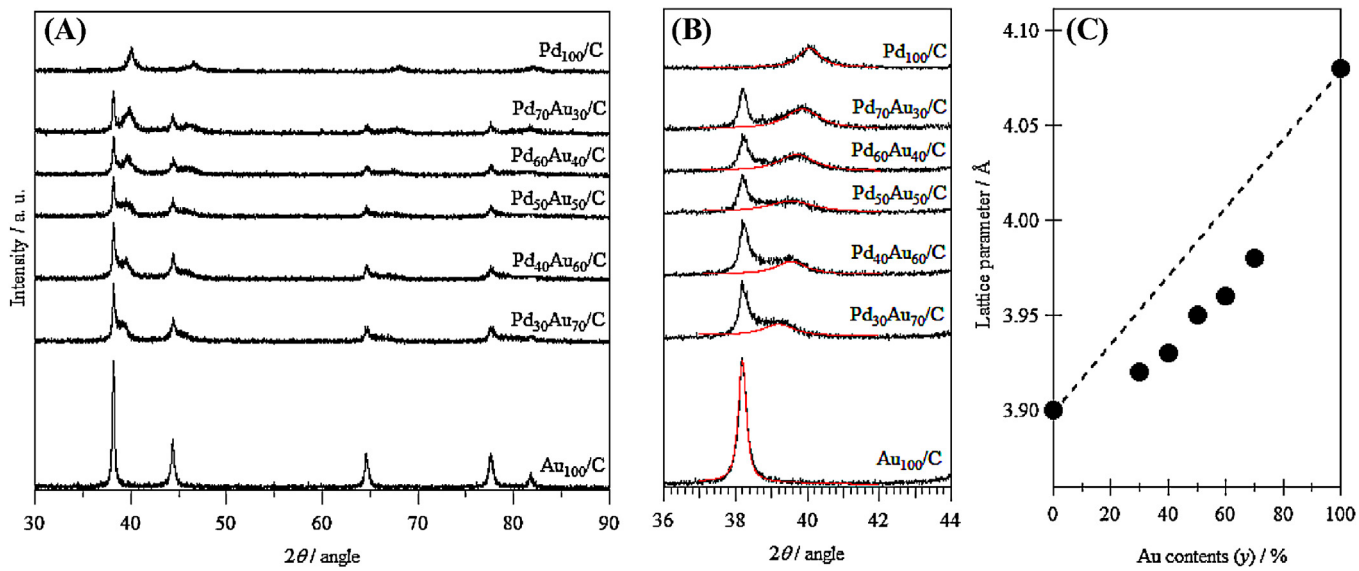

Fig. 4. Analyses of XRD patterns of the Pd_xAu_y/C catalysts. (A) XRD patterns in 30–90° and (B) emphasized detail in 36–44° with the Gaussian fitting (red) of the diffraction derived from PdAu alloy, and (C) estimated values of lattice parameter for Pd_xAu_y/C catalyst as a function of Au contents (y). (For interpretation of the references to color in this legend, the reader is referred to the web version of the article.)

3.3. XRD patterns of Pd_xAu_y/C catalysts

XRD patterns of Pd_xAu_y/C are shown in Fig. 4(A). Both Pd_{100}/C and Au_{100}/C showed the characteristic patterns derived from the face-centered cubic (*fcc*) structure, the reflection peaks were corresponding to the phases for (1 1 1), (2 0 0), (2 2 0), (3 1 1) and (2 2 2) from lower to larger angle. The Pd(1 1 1) plane and the Au(1 1 1) plane were located at $2\theta = 40.06°$ and $2\theta = 38.19°$, respectively, and the lattice parameters were calculated as 3.90 Å from Pd(1 1 1) and 4.08 Å from Au(1 1 1) planes. On the other hand, Pd_xAu_y/C exhibited two patterns on diffractions, one appeared the same positions with Au_{100}/C ($2\theta = 38.19°$) and another located at between that of Au_{100}/C and Pd_{100}/C ($2\theta = 39.86$–$39.20°$). Fig. 4(B) is the emphasized area in $2\theta = 36$–$44°$ of Fig. 4(A) attributing the (1 1 1) diffraction of *fcc* structure. It was reported that the Au@Pd core–shell particles indicated such a humped patterns in this area though the former peak was broader [23]. Thus, the former strong peaks observed at 38.19° supposedly suggested the presence of isolated Au particles in as-prepared Pd_xAu_y/C though which seems to be inactive for selective hydrogenation of HMF to DMF. Moreover, it was observed that the shoulder peaks were gradual shifts to higher angle position with increasing Au contents in Pd_xAu_y/C, though all peaks still sited between the (1 1 1) peaks of Au(1 1 1) plane and Pd(1 1 1) plane. These predicted the presence of PdAu alloy structure in Pd_xAu_y/C. The lattice parameters estimated by the shifting (1 1 1) diffraction peaks of Pd_xAu_y/C were plotted as a function of the introduction amount of Au(y) shown in Fig. 4(c). The correlations between lattice parameter and Au content in Pd_xAu_y/C seems to be linear ($R^2 = 0.98$) but not directly followed with the Vegard's law (the dashed line in Fig. 4(C)), the lattice parameters scale linear between those values for neat Pd and Au by the ratio of the PdAu alloy composition. That is due to contributions of the isolated Au particles in Pd_xAu_y/C, which expected by the strong diffractions attributed to Au particle detected in XRD patterns, included in the horizontal axis in Fig. 4(C). On the basis of the hypothesis that the Pd_xAu_y/C were composed by the isolated Au particles and the homogeneous PdAu alloy particles belonging to the Vegard's law, the compositions of PdAu alloy in Pd_xAu_y/C were estimated by the dash line and the lattice parameter as follows; Pd/Au = 90/10, 81/19, 73/27, 68/32 and 54/46 for $Pd_{70}Au_{30}$/C, $Pd_{60}Au_{40}$/C, $Pd_{50}Au_{50}$/C, $Pd_{40}Au_{60}$/C and $Pd_{30}Au_{70}$/C, respectively.

3.4. XPS spectra of Pd_xAu_y/C catalysts

Fig. 5 illustrated the XPS spectra of Pd_xAu_y/C catalysts in the range of 81–90 eV ascribed to Au 4*f* regions. From a viewpoint of the spectrum of Au_{100}/C, both peaks assigned to Au $4f_{5/2}$ around at 88 eV and $4f_{7/2}$ around at 84 eV showed a gradual shifts to lower side in binding energy with increasing the contents of Pd atoms in Pd_xAu_y/C (Fig. 5(B)). This tendency indicated that the Au atoms gained electrons from Pd atoms by alloying, which is consistent with the higher Pauling's electronegativity of Au (2.54) relative to Pd (2.20), and that was typical in Pd–Au alloying interaction [16,23,31,32]. On the other hands, the XPS spectra derived from Pd $3d_{5/2}$ around at 335 eV and $3d_{3/2}$ around at 340 eV were hard to distinguish there alterations against Au/Pd molar ratio (x/y) because some of them had low intensities and overlapping with the peak of Au $4d_{5/2}$ (Fig. S2). Based on the charge compensation concept, Pd atoms in the Pd_xAu_y/C may have electronic poor states which strongly contributed to the enhancement of activity for hydrogenation reaction of HMF. Previously, importance of Pd^0/Pd^{2+} ratio for a direct synthesis of H_2O_2 from H_2 and O_2 through the H—H bond dissociation and the O—O bond retaining steps over Au@Pd core–shell nanocatalyst have been reported [33,34]. Thus, formation of the electronically poor states in Pd atoms in Pd_xAu_y/C will play a crucial role in the activation of H_2 molecules and/or the enhancement of reaction pathway of hydrogenation, leading to the high activity [30].

3.5. XAFS analyses of Pd_xAu_y/C catalysts

XAFS spectra were measured to further clarify the existence of PdAu alloy on the Pd_xAu_y/C. Fig. 6(A) shows Au L_3-edge XANES spectra of Pd_xAu_y/C. The white-line (WL) feature in Au L_3-edge XANES related to the electron transition from 2*p* to 5*d* electronic states, *i.e.* a higher density in 5*d* state makes a lower intensity in the WL feature. As shown in Fig. 5(A), the WL intensities of Pd_xAu_y/C observed around at 11.92 keV were lower than that of Au foil regardless of Au/Pd molar ratio (x/y), it indicated that the negatively charged Au

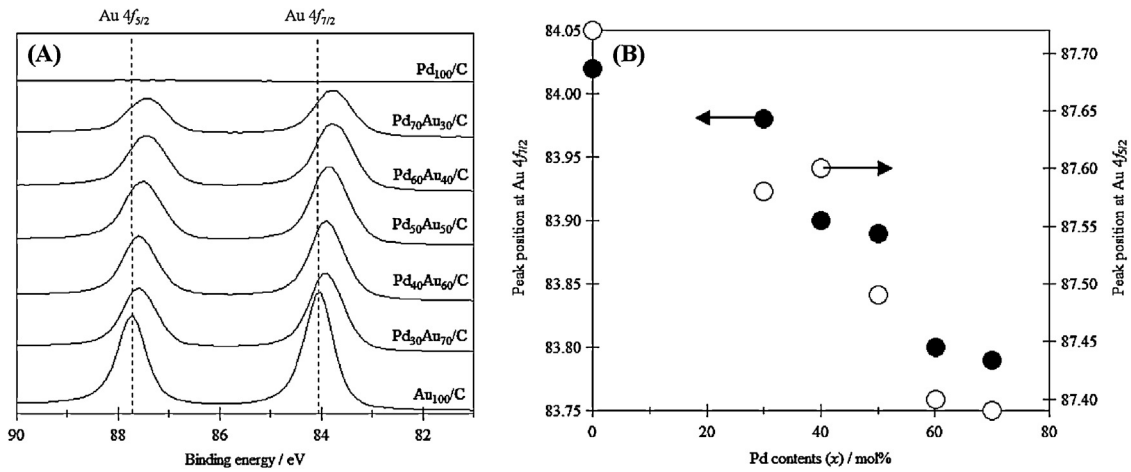

Fig. 5. (A) XPS spectra of the Pd_xAu_y/C catalysts around at Au 4*f* states and (B) plots of the peak positions in Au $4f_{5/2}$ and $4f_{7/2}$ as function of Pd contents (*x*).

5*d* states were appeared in Pd_xAu_y/C *via* charge transfer from Pd to Au. Thus, it strongly suggested that there were electronic interactions between Au and Pd atoms in Pd_xAu_y/C. Pd *K*-edge XANES spectra of Pd_xAu_y/C showed the two-humped features similar to the Pd foil (Fig. S3).

The |FT|s of Au L_3-edge EXAFS spectra were also investigated in Fig. 6(B) [35]. The Au foil and Au_2O_3 exhibited a single peak due to the Au–Au and Au–O coordination with a fitting parameter of 2.84 and 2.01 Å, respectively [36]. While, Pd_xAu_y/C showed intense doublet peaks at 2.11 and 2.95 Å in |FT|s. This splitting arises from the interference between Au–Au and Au–Pd in EXAFS oscillations because the phase shift of Au–Au and Au–Pd are π radian different from each other, though their corresponding distances are expected to be the same. In other word, the appearance of this feature is an obvious support for the presence of Au–Pd interactions in Pd_xAu_y/C. These double peaks were similar to the previous reports about Au@Pd core–shell and random AuPd alloy structure [18,23,37,38]. The |FT|s of Pd *K*-edge EXAFS spectra also described in Fig. 7 [35]. The peak in the range of 2–3 Å gradually splitted into the double with increasing the Au contents in Pd_xAu_y/C [36]. This behavior proposed that the frequency of Pd–Au coordination and/or nanostructure of PdAu alloy will be influenced by Au/Pd molar ratio. With comparing of |FT|s in both Au L_3-edge and Pd *K*-edge, the local structure around Au atoms were much influenced by Pd addition, however the inference of Au progressively increased into Pd atoms.

In the previous literatures, it has been reported that the PdAu bimetallic particle prepared by a simultaneous reduction method at low temperature easily formed Au@Pd core–shell structure due to differences in the reduction potential, $E^0(Pd^{2+}/Pd^0) = +0.63$ V, $E^0(Au^{3+}/Au^0) = +1.0$ V v.s. NHE, and the formation energy [39,40]. Especially, Toshima et al. proposed that the possible nanostructures were cluster-in-cluster, Au@Pd core–shell or random models in the case of Au/Pd = 1/1 with $CN_{Au-Pd} = CN_{Pd-Au}$, while Au@Pd core–shell or random models in the case of Au/Pd = 1/4 with $CN_{Au-Pd} > CN_{Pd-Au}$ [41,42]. Thus, a simple simultaneous EXAFS curve-fitting procedure using a McKale method [43] was conducted

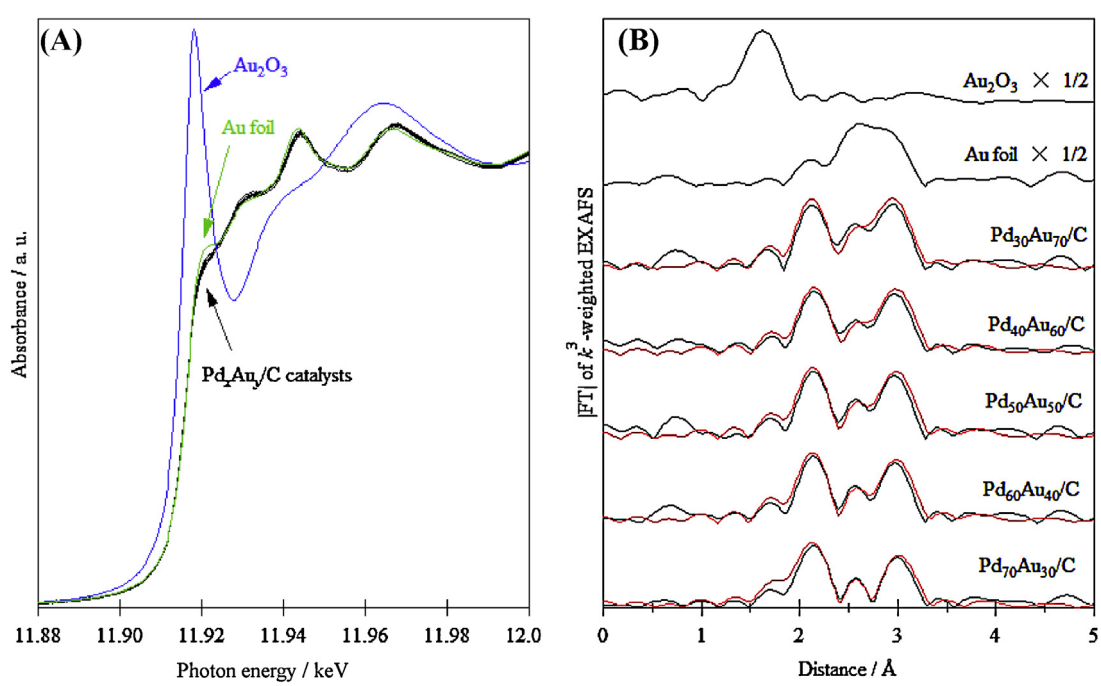

Fig. 6. (A) Au L_3-edge XANES spectra and (B) |FT|s of Au L_3-edge EXAFS spectra of the Pd_xAu_y/C catalysts, Au foil and Au_2O_3 references (black, green and blue solid lines) with the McKale fitting (red solid lines). (For interpretation of the references to color in this legend, the reader is referred to the web version of the article.)

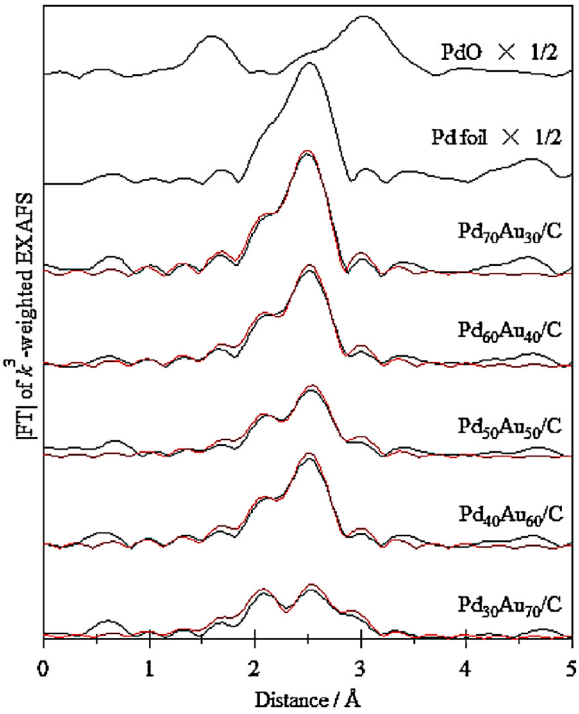

Fig. 7. |FT|s of Pd *K*-edge EXAFS spectra of the Pd_xAu_y/C catalysts, Pd foil and PdO references (black solid lines) with the McKale fitting (red solid lines). (For interpretation of the references to color in this legend, the reader is referred to the web version of the article.)

for bimetallic Pd_xAu_y/C to further challenge for distinguishing their nanostructures. The estimated |FT| patterns were shown in Figs. 6(B) and 7 by red lines, and each fitting parameters were listed in Table S2.

Focusing on the coordination numbers (CN), three bimetallic catalysts of $Pd_{60}Au_{40}/C$, $Pd_{50}Au_{50}/C$ and $Pd_{40}Au_{60}/C$ showed almost equal (2.3–2.9) between CN_{Au-Pd} and CN_{Pd-Au}. For a homogeneous Pd–Au alloy, the ratio of CN_{Pd-Au}/CN_{Pd-Pd} should be equal to the Pd/Au molar ratio, however, the CN_{Pd-Au}/CN_{Pd-Pd} values among these were approximately 0.5 which were smaller than Pd/Au molar ratios estimated by XRD. On the other hand, in the cases of $Pd_{70}Au_{30}/C$ and $Pd_{30}Au_{70}/C$, CN_{Au-Pd} (4.1) > CN_{Pd-Au} (1.6) and CN_{Pd-Au} (4.1) > CN_{Au-Pd} (1.5) were estimated. Consequently, we supposed that $Pd_{60}Au_{40}/C$, $Pd_{50}Au_{50}/C$ and $Pd_{40}Au_{60}/C$ were composed by cluster-in-cluster, Au@Pd core–shell and/or random whereas $Pd_{70}Au_{30}/C$ and $Pd_{30}Au_{70}/C$ were core–shell and/or random. Though further EXAFS investigations are required to determine the detailed information about their nanostructures, we strongly confirmed that the interaction between Pd and Au atoms derived from alloying assigned to a significant catalysis over Pd_xAu_y/C for hydrogenation of HMF toward DMF.

3.6. TEM analyses of $Pd_{50}Au_{50}/C$ catalyst

To further investigate the nanoscale morphology in Pd_xAu_y/C, TEM and STEM-HAADF image with an EDS elemental analysis were measured for $Pd_{50}Au_{50}/C$. Fig. 8(A) indicated that a lot of nanoparticles with average diameter around at 7.5 nm were formed on carbon support [44]. The STEM-HAADF image a particle of 7.1 nm shown in Fig. 8(B) had no contrast. When the AuPd/C was composed by cluster-in-cluster and/or core–shell, the STEM-HAADF image showed bright dark contrast since the heavier element (Au; atomic number, $Z = 79$) gave a brighter image than the lighter (Pd; $Z = 46$) element. Thus, as-synthesized PdAu/C was composed by homogeneous and/or random PdAu alloy. This suggestion is strongly supported by EDS elemental analysis of a particle shown in Fig. 8(C), which exhibited the presence of homogeneously-mixed Pd and Au atoms on the $Pd_{50}Au_{50}/C$. Moreover, the chemical and physical properties in $Pd_{50}Au_{50}/C$ were scarcely changed before and after reaction analyzed by XRD, XPS and TEM techniques (see Figs. S7 and S8).

3.7. Direct synthesis of DMF from fructose and a further application for furfural hydrogenation reaction

We further investigated the synthesis of DMF from fructose and tagatose, a dehydration reaction of these ketoses proceeded over acid catalyst and it served HMF [45]. In our catalytic system, the co-catalyst of HCl will act as the acidic catalyst for dehydration process. In fact, 40% and 10% yields of DMF were produced over PdAu/C catalyst from fructose and tagatose, respectively, in the same reaction conditions (Scheme 2) [46]. Dehydration of fructose was easier than tagatose became the difference position of hydroxyl functional group in C-4 (epimer), thus the yield of DMF from tagatose seems to be lower than that from fructose [47]. Moreover, the hydrogenation of furfural, one of the related reactions [48–50], was also tested over PdAu/C catalyst, it produced 42% yield of 2-MF at 60 °C [51]. These advanced and derivative reactions of furanic compounds are currently ongoing to reveal the novel catalysis of the hydrogenation reaction over the present bimetallic PdAu/C catalyst (Scheme 3).

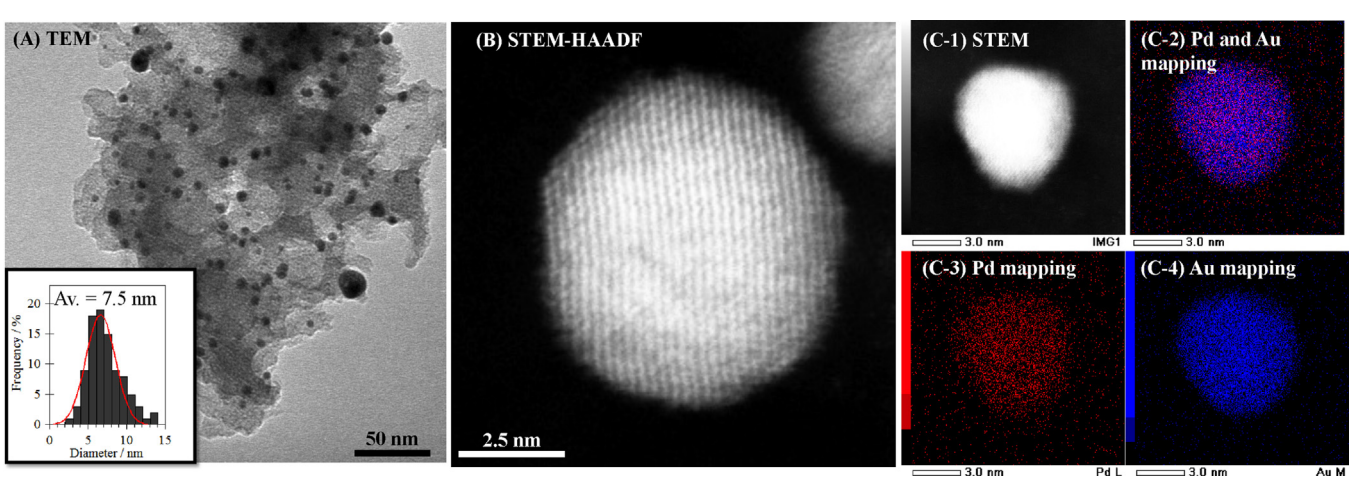

Fig. 8. (A) TEM and (B, C) STEM-HAADF images with an EDS elemental mapping analysis of $Pd_{50}Au_{50}/C$.

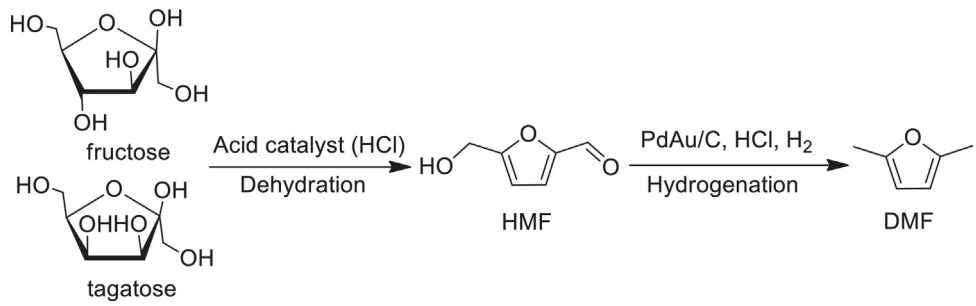

Scheme 2. Direct synthesis of DMF from ketoses.

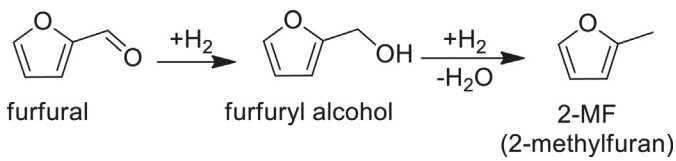

Scheme 3. Hydrogenation of furfural to 2-MF.

4. Conclusions

The PdAu/C catalyst prepared with a simultaneous reduction method exhibited a higher activity than that of Pd/C, Au/C and physical mixture of Au/C and Pd/C for hydrogenation of HMF to DMF under ambient conditions. The XRD patterns indicated that the catalysts were composed by isolated Au particles and PdAu alloy particles. XPS peaks attributed to Au 4*f* states and Au L_3-edge XANES spectra suggested the negatively charged Au atoms were produced with the co-existence of Pd atoms in PdAu/C. EXAFS analyses in both Au L_3-edge and Pd *K*-edge also supported the direct Au–Pd interaction in the PdAu/C. According to these results, we concluded that the AuPd alloy particles stabilized on carbon support possessed a significant activity for the hydrogenation of HMF toward DMF using an atmospheric H_2 gas. Additionally, the PdAu/C exhibited good activities for a direct synthesis of DMF from ketoses in the presence of HCl acidic media and hydrogenation of furfural toward 2-MF.

Acknowledgements

The work was supported by a Grant-in-Aid for Young Scientists (B) (No. 25820392) and Scientific Research (C) (No. 25420825) of the Ministry of Education, Culture, Sports, Science and Technology (MEXT), Japan. Au L_3-edge and Pd *K*-edge XAFS measurements were performed at a BL01B1 of SPring-8 by the approval of the Japan Synchrotron Radiation Research Institute (JASRI) with proposal No. 2012B1610 and a BL5S1 of Aichi Synchrotron Radiation Research Center (2nd period, 2013). The STEM-HAADF image with a EDS elemental mapping analysis was conducted in JAIST supported by Nanotechnology Platform Program of the Ministry of Education, Culture, Sports, Science and Technology (MEXT), Japan. We appreciate Dr. Kohichi Higashimine (Center for Nano Materials and Technology, JAIST) for his great help of STEM-HAADF and EDS elemental mapping analysis.

Appendix A. Supplementary data

Supplementary data associated with this article can be found, in the online version, at http://dx.doi.org/10.1016/j.cattod.2013.10.012.

References

[1] Annual Energy Outlook 2013 (AEO2013), the U.S. Energy Information Administration (EIA), Washington, DC, 2013.
[2] G.W. Huber, S. Iborra, A. Corma, Chem. Rev. 106 (2006) 4044.
[3] D.M. Alonso, J.Q. Bond, J.A. Dumesic, Green Chem. 12 (2010) 1493.
[4] K. Wilson, A.F. Lee (Eds.), Handbook of Heterogeneous Catalysts for Clean Technology: Design, Analysis and Application, first ed., Wiley-VCH, Weinheim, Germany, 2013.
[5] R.-J. van Putten, J.C. van der Waal, E. de Jong, C.B. Rasrendra, H.J. Heeres, J.G. de Vries, Chem. Rev. 113 (2013) 1499.
[6] Y. Roman-Leshkov, C.J. Barrett, Z.Y. Liu, J.A. Dumesic, Nature 447 (2009) 982.
[7] M. Chidambaram, A.T. Bell, Green Chem. 12 (2010) 1253.
[8] J. Ohyama, A. Esaki, Y. Yamamoto, S. Arai, A. Satsuma, RSC Adv. 3 (2013) 1033.
[9] R. Alamillo, M. Tucker, M. Chia, Y. Pagan-Torresa, J. Dumesic, Green Chem. 14 (2012) 1413.
[10] W. Yang, A. Sen, ChemSusChem 3 (2010) 597.
[11] G.C.A. Luijkx, N.P.M. Huck, F. van Rantwijk, L. Maat, H. van Bekkum, Heterocycles 77 (2009) 1037.
[12] T. Thananatthanachon, T.B. Rauchfuss, Angew. Chem. Int. Ed. 49 (2010) 6616.
[13] T.B. Rauchfuss, T. Thananatthanachon, US Patent Application, US 2011/02638801 A1.
[14] S. De, S. Dutta, B. Saha, ChemSusChem 5 (2012) 1826.
[15] D.I. Enache, J.K. Edwards, P. Landon, B. Solsona-Espriu, A.A. Herzing, M. Watanabe, C.J. Kiely, D.W. Knight, G.J. Hutchings, Science 311 (2006) 362.
[16] S. Nishimura, Y. Yakita, M. Katayama, K. Higashimine, K. Ebitani, Catal. Sci. Technol. 3 (2013) 351.
[17] A. Villa, M. Schiavoni, S. Campisi, G.M. Veith, L. Prati, ChemSusChem 6 (2013) 609.
[18] T. Balcha, J.R. Strobl, C. Fowler, P. Dash, R.W.J. Scott, ACS Catal. 1 (2011) 425.
[19] J.K. Edwards, B. Solsona, E. Ntainjua, A.F. Carley, A.A. Herzing, C.J. Kiely, G.J. Hutchings, Science 323 (2009) 1037.
[20] J.K. Edwards, E. Ntainjua, A.F. Carley, A.A. Herzing, C.J. Kiely, G.J. Hutchings, Angew. Chem. Int. Ed. 48 (2009) 8512.
[21] P.-P. Fang, A. Jutand, Z.-Q. Tian, C. Amatore, Angew. Chem. Int. Ed. 50 (2011) 12184.
[22] J. Xu, A.R. Wilson, A.R. Rathmell, J. Howe, M. Chi, B.J. Wiley, Nano Lett. 5 (2011) 6119.
[23] X. Yuan, G. Sun, H. Asakura, T. Tanaka, X. Chen, Y. Yuan, G. Laurenczy, Y. Kou, P.J. Dyson, N. Yan, Chem. Eur. J. 19 (2013) 1227.
[24] A surface area was analyzed by N_2 adsorption at 77 K with BELSORP-max.
[25] M. Brandalise, M.M. Tusi, R.M. Piasentin, M.C. dos Santos, E.V. Spinace, A.O. Neto, Int. J. Electrochem. Sci. 7 (2012) 9609.
[26] Supposed to be decomposed during GC-FID analysis.
[27] N. Nikbin, S. Caratzoulas, D.G. Vlachos, ChemSusChem (2013) (in press).
[28] L. Bui, H. Luo, W.R. Gunther, Y. Roman-Leshkov, Angew. Chem. Int. Ed. 52 (2013) 8022.
[29] J.-P. Lange, E. van der Heido, J. van Buijtenen, R. Price, ChemSusChem 5 (2012) 150.
[30] Reactivities of the adsorbed aldehyde and hydroxylalkyl groups in furanic compounds and/or H_2 species on Pd surface were supposedly influenced by the Pd condition. Further investigations of the electronic state of Pd atoms and their contribution onto the reaction mechanism are now on going.
[31] F. Liu, D. Wechsler, P. Zhang, Chem. Phys. Lett. 461 (2008) 254.
[32] P.A.P. Nascente, S.G.C. de Castro, R. Landers, G.G. Kleiman, Phys. Rev. B 43 (1991) 4659.
[33] M. Piccinini, E. Ntainjua, J.K. Edwards, A.F. Carley, J.A. Moulijn, G.J. Hutchings, Phys. Chem. Chem. Phys. 12 (2010) 2488.
[34] J. Pritchard, M. Piccinini, R. Tiruvalam, Q. He, N. Dimitratos, J.A. Lopez-Sanchez, D.J. Morgan, A.F. Carley, J.K. Edwards, C.J. Kiely, G.J. Hutchings, Catal. Sci. Technol. 3 (2013) 308.
[35] The corresponding EXAFS spectra were shown in Fig. S4.
[36] Monometalic Au/C or Pd/C indicated a similar peak to Au foil or Pd foil in |FT| shown in Fig. S5.
[37] P. Dash, T. Bond, C. Fowler, W. Hou, N. Coombs, R.W.J. Scott, J. Phys. Chem. C 113 (2009) 12719.

[38] M.R. Knecht, M.G. Weir, A.I. Frenkel, R.M. Crooks, Chem. Mater. 20 (2008) 1019.
[39] S. Okada, K. Fujiwara, T. Kamegawa, K. Mori, H. Yamashita, Bull. Chem. Soc. Jpn. 85 (2012) 1057.
[40] H.B. Liu, U. Pal, A. Medina, C. Maldonado, J.A. Ascencio, Phys. Rev. B 71 (2005) 075403.
[41] N. Toshima, M. Harada, Y. Yamazaki, K. Asakura, J. Phys. Chem. 96 (1992) 9927.
[42] N. Toshima, T. Yonezawa, New J. Chem. 22 (1998) 1179.
[43] A.G. McKale, B.W. Veal, A.P. Paulikas, S.-K. Chan, G.S. Knapp, J. Am. Chem. Soc. 110 (1988) 3763.
[44] In some cases, the agglomerates shown in Fig. S6 were also observed but we ignored these particles.
[45] J. Tutejya, S. Nishimura, K. Ebitani, Bull. Chem. Soc. Jpn. 85 (2012) 275.
[46] Reaction conditions; ketose (0.5 mmol), THF (10 ml), HCl (0.17 mmol), $Pd_{40}Au_{60}$/C (31.3 mg), H_2 balloon (purge), 60 °C, 12 h.
[47] Direct synthesis of DMF from aldoses such as glucose and galactose using the same reaction conditions did not proceed (0% yields), because the dehydration reaction of aldoses needs a higher temperature than that of ketoses, normally.
[48] Y. Nakagawa, H. Nakazawa, H. Watanabe, K. Tomishige, ChemCatChem 4 (2012) 1791.
[49] S. Sitthisa, T. Pham, T. Prasomsri, T. Sooknoi, R.G. Mallinson, D.E. Resasco, J. Catal. 280 (2011) 17.
[50] S. Sitthisa, D.E. Resasco, Catal. Lett. 141 (2011) 784.
[51] Reaction conditions; furfural (1.0 mmol), THF (10 ml), HCl (0.17 mmol), $Pd_{40}Au_{60}$/C (31.3 mg), H_2 balloon (purge), 60 °C, 12 h.